Polymer 50 (2009) 5613–5617

Contents lists available at ScienceDirect

Polymer

journal homepage: www.elsevier.com/locate/polymer

A mesoscopic network model for permanent set in crosslinked elastomers

Todd H. Weisgraber [a,*], Richard H. Gee [a], Amitesh Maiti [a], David S. Clague [b], Sarah Chinn [a], Robert S. Maxwell [a]

[a] Lawrence Livermore National Laboratory, 7000 East Avenue L-184, Livermore, CA 94551, USA
[b] Department of Biomedical Engineering, California Polytechnic State University, San Luis Obispo, CA 93407, USA

ARTICLE INFO

Article history:
Received 19 February 2009
Received in revised form
16 September 2009
Accepted 16 September 2009
Available online 20 September 2009

Keywords:
Polymer physics
Polydimethylsiloxane
Aging

ABSTRACT

A mesoscopic computational model for polymer networks and composites is developed as a very coarse-grained representation of the network microstructure. Unlike more complex molecular dynamics simulations, the model network is static unless undergoing deformation. The elastic modulus, which depends only on the crosslink density and parameters in the bond potential, is consistent with rubber elasticity theory, and the network response satisfies the independent network hypothesis of Tobolsky. The model, when applied to a commercial filled silicone elastomer, quantitatively reproduces the experimental permanent set and stress-strain response due to changes in the crosslinked network from irradiation.

1. Introduction

Filled polymeric composites have numerous applications in science, engineering, and medicine due to their many advantageous properties, including thermal stability, chemical inertness, and biocompatibility [1,2]. Over time, changes in the network microstructure due to chemical bond scission and crosslinking can alter these properties [3,4]. In particular, chemical aging can strongly affect the elastic properties of the network through modifications to the network as well as changes in the interactions between the polymer and filler particles. Furthermore, changes in the mechanical properties can depend on the strain history. For example, an elastomer that undergoes additional crosslinking in a state of strain can acquire a permanent set or deformation when the applied stress is removed [5,6].

In many instances, polymeric materials serve as critical components, so, developing accurate models to predict lifetime performance in different environments is essential. To describe permanent set, Tobolsky first hypothesized that new crosslinks introduced in a state of strain are independent of the original network formed by crosslinking at zero strain [7]. Thus, the stress of the material is a linear combination of the contributions from both networks. This independent network hypothesis can be used in conjunction with a variety of constitutive relations from rubber elasticity theory, including the affine network model and more sophisticated approaches like the slip-tube model [8]. Comparisons of these approaches with molecular dynamics (MD) simulations have shown varying degrees of success in predicting permanent set [5,9].

In realistic aging scenarios, elastomeric networks undergo both crosslinking and scission and a modification to the independent network hypothesis is required. For the sequential case of forming a second network by crosslinking while in a state of deformation, followed by scission of the original network, the concept of a stress transfer function was introduced [10,11]. Physically, this function accounts for the fraction of the second network that reinforces the original, and the crosslink densities in the Tobolsky model are replaced by effective crosslink densities that incorporate the stress transfer function. Rottach et al. compared the fractional stress reduction after scissioning the original network, as computed by molecular dynamics, to predictions of the slip-tube model incorporating the stress transfer function [12]. Recently we demonstrated the effectiveness of the Fricker stress transfer function in reproducing permanent set data from experiments with artificially aged filled siloxane composites [13].

In this investigation, we propose a different approach. Since it is difficult to derive a theory that can predict macroscopic stresses from microstructural deformations, many of the predictive constitutive equations are phenomenological or empirical in nature. In an effort to increase the amount of coarse-graining in molecular representations, we have developed a mesoscopic numerical model

* Corresponding author. Lawrence Livermore National Laboratory, 7000 East Avenue L-184, Livermore, CA 94551, USA. Tel.: +1 925 423 6349.
E-mail address: weisgraber2@llnl.gov (T.H. Weisgraber).

0032-3861/$ – see front matter © 2009 Elsevier Ltd. All rights reserved.
doi:10.1016/j.polymer.2009.09.046

that incorporates some details of the microstructure without resorting to computationally intensive MD calculations, while maintaining the functionality and predictability required for engineering applications. Similar physics-based models have appeared in the literature. Arruda and Boyce proposed an eight chain network model to reproduce the stress response of elastomers for several types of deformation [14]. Hanson developed a model for filled and unfilled polydimethylsiloxane (PDMS) by physically modeling a small fraction of the polymer chains in a given volume [15], where the polymer intra-chain forces and polymer-filler forces were based on more detailed MD simulations. In our numerical model presented here, large sections of the polymer chains are coarse-grained to a single bond since we are interested in the equilibrium response prior to and during the aging process. We validated the predictability of the model by comparing with experimental aging data, which characterized the stress response, changes in the crosslink density, and permanent set of a filled PDMS elastomer [16].

2. Model description

The mesoscopic network model consists of sets of "bonded" nodes, which may represent crosslinks, entanglements, or filler particles in the material. In this work selected node pairs are linked by a single "bond", which represents the entire polymer chain between crosslinks in the network. Initially the connectivity was arranged on a simple cubic lattice with periodic boundary conditions so that each node had a coordination number or maximum connectivity of six. The bond interactions are described by a FENE spring potential, given by [17]

$$V_{\mathrm{FENE}}(r) = -\frac{1}{2}kR_0^2\ln\left[1-\left(\frac{r}{R_0}\right)^2\right], \quad r < R_0 \tag{1}$$

where k is the spring constant and R_0 is the maximum extension. To stabilize the network at large extensions, a standard Lennard-Jones (12-6) potential,

$$V_{\mathrm{LJ}}(r) = 4\varepsilon\left[\left(\frac{\sigma}{r}\right)^{12}-\left(\frac{\sigma}{r}\right)^{6}\right]+\varepsilon, \quad r \le 2^{1/6}\sigma$$
$$= 0, \quad r > 2^{1/6}\sigma \tag{2}$$

was incorporated between bonded nodes.

Bonds within the initial cubic lattice were randomly selected and deleted from the lattice to obtain the desired connectivity, typically corresponding to a network with no more than a tetrafunctional junction at each node, in a manner similar to Grimson [18]. The ensemble of bonded nodes was then relaxed via energy minimization to obtain the initial structure, where the volume was adjusted to enforce an isotropic pressure constraint on the relaxed state. Therefore, the resulting domain was not a perfect cube but a slightly rectangular box. It is also possible to generate the network by randomly placing nodes within a cubic domain and introducing sufficient bonds between neighbors to produce the desired number of crosslinks.

The deformation and response of the network model was computed with the LAMMPS parallel molecular dynamics code [19]. For this initial evaluation of the model we limited our tests to uniaxial extensions to mimic the experiments of Chinn et al. [16]. Our molecular simulations were static without thermal fluctuations, and consisted of a series of small deformations, followed by an energy minimization step to obtain the equilibrium node positions for the applied deformation. The networks were deformed by stretching the domain along the x-axis from L_x to λL_x at a constant volume so the lateral dimensions were contracted by a factor of $\lambda^{-1/2}$, where λ is the extension ratio. The energy minimization step ensured that the net force on each node was near zero. We compared the network stress responses for different energy and force tolerances to ensure these values were small enough to allow the model to reach equilibrium. The stress response in the direction of extension is equivalent to the deviatoric part of the stress tensor, $\sigma_{xx} = 3/2(P_{xx} - 1/3\sum_i P_{ii})$, computed during the simulation, where the coefficient of 3/2 arises from the constant volume constraint [5], and the second term in the parenthesis is the hydrostatic pressure.

In this work, we varied the parameters k and R_0 in Equation (1) to fit experimental results and fixed $b = (3/2)\sigma$ and $\varepsilon = k/30$, where b is the initial bond length between nodes. We selected a cubic lattice with 16 nodes per dimension for a total of 4096 sites. Preliminary calculations revealed the stress response was independent of the node number for networks with eight or more nodes per dimension. Larger networks with more nodes are more robust at higher deformations where the bonds are stretched close to their maximum extension. Since we were essentially computing a series of static configurations, an extension/compression calculation could run on a single processor and required no more than a few minutes to complete.

3. Results and discussion

3.1. Single-stage network model

We performed a set of parametric studies to evaluate the response of the network model to the adjustable parameters. Since the FENE bond potential depends linearly on k, we expected a linear relationship between it and the computed stress. Furthermore, we expected that the stress and system size, expressed as $L_x = 24\sigma$, are inversely proportional. To verify these claims, we computed the stress response to uniaxial stretch for a variety of networks with a wide range of k and L_x values. In Fig. 1, which shows the normalized engineering stress for selected networks with a fixed crosslink density and $R_0 = 2.5\sigma$, all the curves nicely collapse, confirming the linear relationship between stress and k and L_x^{-1} over a large range of uniaxial deformations. The upswing in the stress is due to the finite extensibility. In the small strain limit the network recovered the behavior of the phantom network model [20], and produced a constant shear modulus. However at very small strains

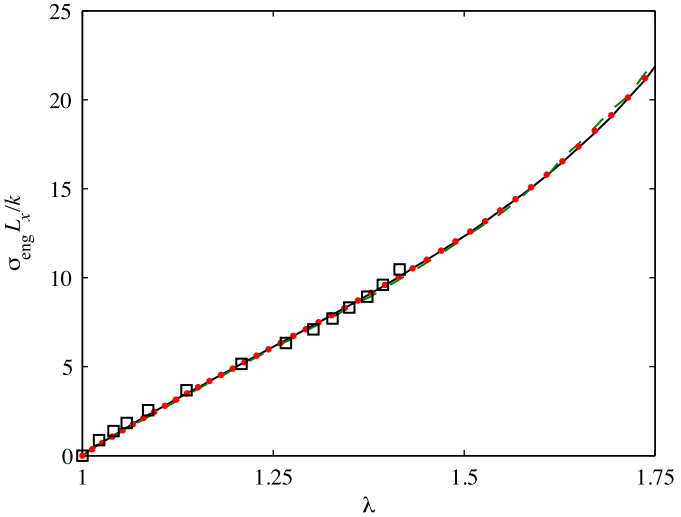

Fig. 1. Normalized engineering stress ($\sigma_{\mathrm{eng}} = \sigma_{xx}/\lambda$) for networks with different values of k and L_x: $k/L_x = 91.9$ kPa (solid black line), $k/L_x = 998.7$ kPa (dashed green line), and $k/L_x = 45.2$ kPa (red circles) ($R_0 = 2.5\sigma$). The squares are the experimental values of the DC-745 response from Chinn et al. [16]. (For interpretation of the references to colour in this figure legend, the reader is referred to the web version of this article.)

($\lambda < 1.03$), the model exhibited some non-linear behavior, likely due to the Lennard-Jones contribution.

To test the robustness of the model, we generated three different network ensembles by removing a different set of random bonds from the initial cubic lattice and compared the stress response of each ensemble using the same k and L_x values. For the range of deformations in Fig. 1, the ensemble standard deviation for the stress was 1.2% of the ensemble average. Therefore the results were quite repeatable for different network realizations.

Networks with varying crosslink densities were created by changing the number of initial bonds in the lattice, as described in the previous section. Since the number of nodes (or crosslink sites) remains constant, this physically corresponds to changing the polymer density or number of chains, which is proportional to the crosslink density. Another way to express the crosslink density in the domain is by the ratio of the number of bonds to the total bonds available in the network, referred to herein as the conversion, p. In the initial cubic lattice the total number of initial bonds before depletion was three times the number of nodes. Rubber elasticity theory predicts that stress is proportional to $p - p_{gel}$, where p_{gel} is the conversion ratio at the gel point, since the bonds formed below the gel point do not contribute to the elastic response. The gel point for this network model should be approximately equal to the percolation bond threshold for a simple cubic lattice, or 0.25 [21]. To test this assumption, we computed the stress at an extension ratio of 1.4 for networks with crosslink densities near the percolation threshold and defined the gel point where the stress had a sharp transition from near zero to non-zero values. As indicated in the inset of Fig. 2, we estimated the gel point to be $p_{gel} = 0.29$, a value slightly higher than the theoretically predicted cubic lattice percolation threshold.

We also tested the response for crosslink densities above the gel point, and the final stresses at $\lambda = 1.4$ are plotted in Fig. 2 as a function of both the relative conversion ratio, which is proportional to crosslink density, and R_0. For large R_0, the relationship between stress and crosslink density is linear, consistent with rubber elasticity theory [5]. However, for smaller R_0, the relationship becomes non-linear due to the finite extension effects of Eq. (1), which manifested as an upswing in the stress-elongation response curve.

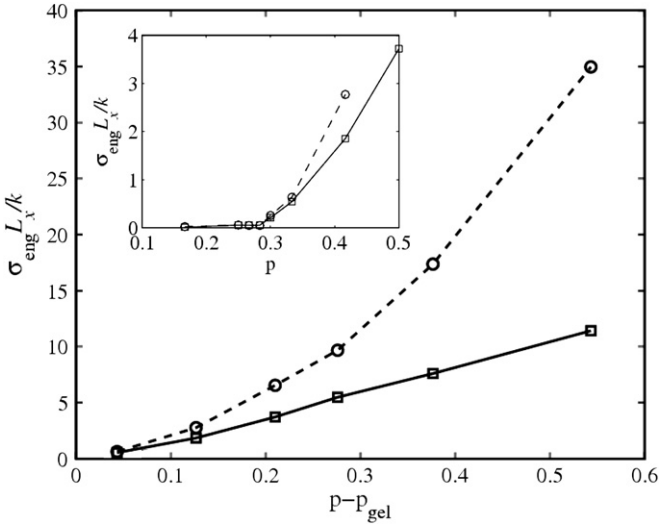

Fig. 2. Engineering normalized stress of the network model at a strain state of $\lambda = 1.4$ for different relative conversion ratios, p, and maximum bond extensions. The squares correspond to networks with $R_0 = 10\sigma$, and the circles correspond to networks with $R_0 = 2.5\sigma$. The inset figure shows the network responses as a function of absolute conversion ratio to determine the value of $p_{gel} = 0.29$.

3.2. Two-stage network model

To simulate material damage from radiation, the network was modified through a series of bond breaking (scission) and formation (crosslinking) steps. With the system in a strained state, we first performed a scission step, in which bonds were randomly selected and deleted from the network. Next, in the crosslinking step, a node with less than six bonds was randomly selected and a list of its neighboring nodes within a certain cutoff distance and having less than six bonds was generated. After randomly selecting from this neighbor list, a bond was then formed between the two selected nodes. Finally, this new network configuration was relaxed via energy minimization to its new static configuration. Note that there is no time scale, or chemical reaction rate, in this process; bond breaking and formation occur instantaneously.

To evaluate the predictability of the model, we compared our results to experiments performed by Chinn et al. [16], who exposed samples of commercial, filled siloxane elastomer (DC-745) under uniaxial strain to controlled dosages of γ-radiation from a Co-60 source. After removing the applied strain, the permanent set and stress response of the aged samples were measured. Nuclear magnetic resonance (NMR) and swelling experiments were also conducted to determine the net change in crosslink density. Crosslinking reactions were more prevalent than scission during the exposure to γ-radiation and the change in density was independent of the stretch ratio, λ_1.

By fitting the experimental data with a two-stage network model and the Mooney-Rivlin materials equation, we established a linear relationship between the applied radiation dosage and the fraction of chain scissioning, $\xi_{sci} = \nu_{sci}/(\nu_0 - \nu_{gel})$, and new network crosslinks, $\xi_{x1} = \nu_1/(\nu_0 - \nu_{gel})$, relative to the initial crosslink density, ν_0, where ν_1 is the crosslink density of the second network, and ν_{gel} is the gel point crosslink density [13]. Thus we obtained a direct relationship between the change in the number of bonds in the network model and the experimental dosage.

We first considered the case when no scission occurs so the original network is unchanged while a new set of bonds is introduced in the strained state. According to the independent network hypothesis of Tobolsky, the second network is in an unstrained state and therefore should have no contribution to the stress at the stretch ratio in which it is added. Fig. 3 shows the stress prior to and after introducing the second set of crosslinks for various initial conversion ratios, p. The stress response at a new network ratio of zero corresponds to the stress of the original network. The stress remains largely unchanged for all the networks except for the conversion ratio of 0.41 (the highest crosslinking investigated here). There is a slight upward trend in the stress with crosslinking for the two lowest density networks, whereas the higher crosslinked networks exhibit a decreasing trend, both most likely caused by the non-linearity of the springs. However, these changes are small and overall, the results demonstrate the model's consistency with the independent network hypothesis.

Incorporating scission into the model allowed direct comparisons with the experiments of Chinn et al. [16]. We first fit the experimental data for a pristine siloxane sample (square points in Fig. 1) to the normalized stress-strain response using a ratio of $k/L_x = 91.9$ kPa, $R_0 = 2.5\sigma$, and a relative conversion ratio, $p - p_{gel}$ of 0.31. It is apparent that the model captures the correct elastic modulus and somewhat under predicts the extent of the experimental upswing at the highest strain (last point). The upswing in the model curve is less pronounced and occurs at a larger stretch ratio of $\lambda = 1.5$.

We checked the consistency of the model with the k/L_x fitting parameter by independently estimating a spring constant and length scale. The length scale can be obtained by comparing the number of bonds in the model to the crosslink density of the DC-

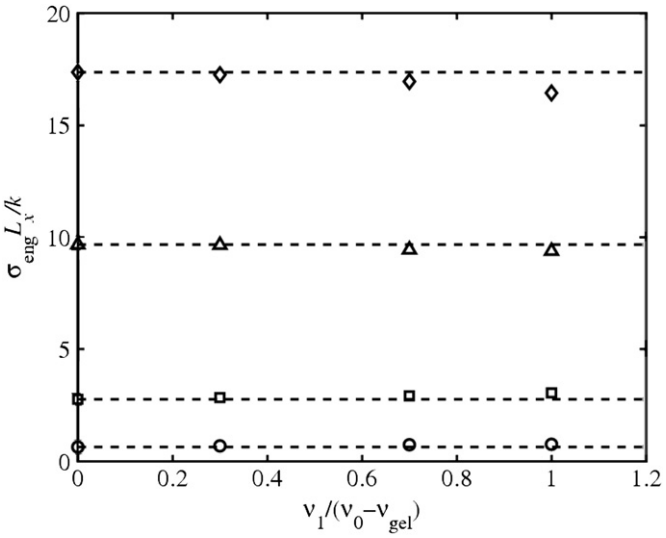

Fig. 3. Engineering stress after networks are crosslinked in a strained state ($\lambda = 1.4$) for different initial crosslink densities and density of second network. The stress at zero radiation dosage is the value prior to adding the second network and is also indicated by the horizontal dashed lines. Symbols correspond to initial conversion ratio, $p_0 - p_{gel}$: 0.073 (circles), 0.16 (squares), 0.31 (triangles), and 0.41 (diamonds). No scission occurs in the data shown here.

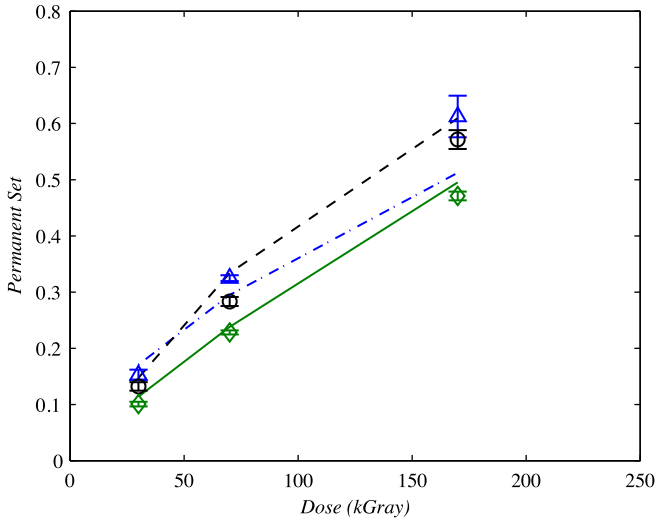

Fig. 4. Permanent set experimental data of Chinn et al. [16] (lines) and model predictions (symbols) for a range of radiation dosages applied at strained states of $\lambda_1 = 1.2$ (blue: triangles and dash-dot line), $\lambda_1 = 1.4$ (black: circles and dashed line), and $\lambda_1 = 1.9$ (green: diamonds and solid line). Error bars indicate the standard deviation for three independent ensembles. (For interpretation of the references to colour in this figure legend, the reader is referred to the web version of this article.)

745 sample. In our previous work [13], we estimated the elastic modulus to be 933 kPa which corresponds to a crosslink density of $2.24 \times 10^8\ \mu m^{-3}$ from the relationship $G \sim \nu_0 kT$. Based on the selected conversion ratio, the network model is then equivalent to a 31 nm cube of this material. The entropic spring constant of an ideal chain is given by $k_{ideal} = 3kT/\langle R^2 \rangle$, where $\langle R^2 \rangle$ is end-to-end distance of the chain. For this estimate, we defined an effective or average network spring constant based on the mean-squared bond distance between crosslinks in the microstructure. From our model this distance is ~1.8 nm and therefore the estimate for k/L_x based on the properties of DC-745 and the physical assumptions in the network is 120 kPa. Considering the amount of coarse-graining in this approach it is encouraging to find the fitted (91.9 kPa) and estimated values of this ratio were within a factor of 1.3.

In addition to the entropic spring behavior of the polymer molecules, the importance of the contribution of entanglements to the shear modulus is well established [22]. Our model does not explicitly account for the latter. However, since the effective spring constant of the bonds in our network was chosen as a best fit to the response of the virgin experimental specimen, the contribution of the entanglements is reflected in this value albeit not explicitly modeled.

With the model parameters set, we calculated the permanent set at radiation dosages, D, at deformations, λ_1, corresponding to the experiments. The amount of scission and crosslinking was related to the radiation dosage using the previously calibrated relationships [13]. The parameters describing the additional bonds in the second network were identical to those in the original network. After the scission, crosslinking, and relaxation steps to incorporate the second network, the domain was gradually compressed, with the previously described intermediate energy minimization steps, to a state of zero stress, thus providing the domain recovery ratio, λ_s. The permanent set was calculated from the definition,

$$P_s = \frac{\lambda_s - 1}{\lambda_1 - 1}. \tag{3}$$

Fig. 4 compares the permanent set predictions from the mesoscopic numerical model and the corresponding experimental values. Each point represents the average of three ensembles of random scission and crosslinking, and the error bars correspond to the standard deviation. Considering the simplicity of the model, the agreement is excellent, with the largest difference of 10% occurring at the 170 kGray dosage. Also note that the model correctly reproduced a decrease in permanent set with increasing λ_1, whereas the experimental data deviated from this behavior at the higher radiation dosages. There may have been some experimental error measuring the permanent set at smaller extensions, however, despite the uncertainty, the range of permanent set is closely matched between the data and the model at each radiation dosage.

In our previous work, we incorporated the Fricker stress transfer function into the Mooney-Rivlin materials model and obtained a good fit to the permanent set data as well [13]. Unlike constitutive models however, the mesoscopic network does not specifically incorporate a stress transfer function, to account for feedback between the first and second network when additional crosslinks are created. Thus, the stress transfer effect is intrinsic to the model and the way the network is modified under tension, which is why the permanent set predictions were comparable to experiment. For example, in this model, when part of the original network undergoes scission in a state of strain, there is a corresponding decrease in stress due to the loss of connectivity. However, when the same amount of scission is applied along with additional crosslinking, the drop in stress is not as large since the second network can accommodate some of the stress. This is precisely the kind of feedback effect described by the stress transfer function. Note that Fig. 3 confirms there is no stress transfer when no scission occurs in the original network. Furthermore, it is worthwhile to note that the parameters in the Mooney-Rivlin two-stage equation were obtained by fitting to the permanent set data, whereas the parameters for this mesoscopic model were solely derived from the stress response of the pristine sample. The permanent set values were predictive.

Finally, we performed additional extension simulations for the modified networks simulating irradiation at 170 kGray to compare the predicted material responses with the experimental samples. As shown in Fig. 5, the agreement at small stretch ratios is excellent and the increasing elastic modulus with decreasing λ_1 is reproduced. At larger deformations, the network model and experiment

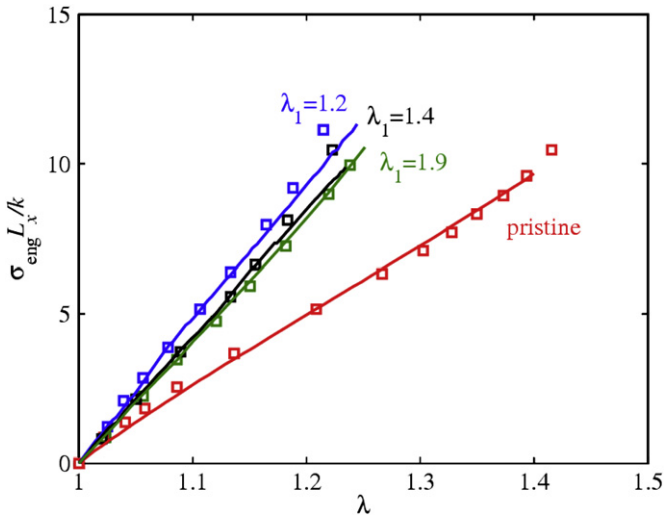

Fig. 5. Normalized stress response of experimental siloxane composite samples of Chinn et al. [16] (squares) after irradiating at 170 kGray at different stretch ratios, λ_1, and response of the mesoscopic model (lines).

deviate, most likely due to finite extensibility effects. Presumably we could improve the model by adjusting the maximum bond extension to better capture the upswing.

4. Conclusions

We have developed a computational mesoscopic model of polymer networks using a very coarse-grained approach that consolidates the segments of the polymer chains between crosslinks into a single bond. By ignoring the dynamics of the chains, only the static configuration of this heterogeneous network contributed to its material properties. Three free parameters, the spring constant, k, maximum bond extension, R_0, and crosslink density or conversion ratio, p, characterized the initial network. For relatively large maximum extensions, the elastic modulus varied linearly with both spring constant and crosslink density; hence, only two free parameters were required to describe the network.

Since there were no underlying dynamics in the network, bonds could be added and removed instantaneously. By first considering only crosslinking, we demonstrated the stress remained constant when adding the second network in a uniaxially strained state and therefore the model was consistent with the independent network hypothesis. Upon fixing the free parameters by fitting the stress response to data for a commercial filled siloxane, the model predicted the amount of permanent set and increase in elastic modulus after exposure to a radiation source. No other assumptions were needed to obtain remarkable agreement with the experimental data, and the network automatically reproduced the effects of stress transfer. These results also indicate that reducing the maximum bond extension may further improve the agreement with experiments at larger deformations. We plan to continue development of this model and will explicitly include the effect of filler particles by creating a heterogeneous bond structure. Comparisons with foams and other filled elastomers are also in progress.

Acknowledgement

This work performed under the auspices of the U.S. Department of Energy by Lawrence Livermore National Laboratory under Contract DE-AC52-07NA27344.

References

[1] Mark JE, Erman B. Rubberlike elasticity: a molecular primer. Cambridge: Cambridge; 2007.
[2] Saltzman WM. Drug delivery: engineering principles for drug therapy. New York: Oxford University Press; 2001.
[3] Tobolsky AV. Properties and structure of polymers. New York: Wiley; 1960.
[4] Curro JG, Salazar EA. J Appl Polym Sci 1975;19:2571–81.
[5] Rottach DR, Curro JG, Grest GS, Thompson AP. Macromolecules 2004;37(14):5468–73.
[6] Andrews RD, Tobolsky AV, Hanson EE. J Appl Phys Chem 1946;17:352–61.
[7] Tobolsky AV, Prettyman IV, Dillon JH. J Appl Phys 1944;15:380–95.
[8] Rubinstein M, Panyukov S. Macromolecules 2002;35(17):6670–86.
[9] Rottach DR, Curro JG, Budzien J, Grest GS, Svaneborg C, Everaers R. Macromolecules 2006;39(16):5521–30.
[10] Flory PJ. Trans Faraday Soc 1960;56(5):722–43.
[11] Fricker HS. P Roy Soc Lond A Mat 1973;335(1602):289–300.
[12] Rottach DR, Curro JG, Budzien J, Grest GS, Svaneborg C, Everaers R. Macromolecules 2007;40(1):131–9.
[13] Maiti A, Gee RH, Weisgraber TH, Chinn S, Maxwell RS. Polym Degrad Stabil 2008;93:2226–9.
[14] Arruda EM, Boyce MC. J Mech Phys Solid 1993;41(2):389–412.
[15] Hanson DE. Polymer 2004;45(3):1055–62.
[16] Chinn S, DeTeresa S, Sawvel A, Shields A, Balazs B, Maxwell RS. Polym Degrad Stabil 2006;91(3):555–64.
[17] Kremer K, Grest GS. J Chem Phys 1990;92(8):5057–86.
[18] Grimson MJ. Mol Phys 1991;74(5):1097–114.
[19] Plimpton SJ. Comp Phys 1995;117(1):1–19.
[20] James HM, Guth E. J Chem Phys 1943;11(10):455–81.
[21] Lorenz CD, Ziff RM. Phys Rev E 1998;57(1):230–6.
[22] Everaers R, Sukumaran SK, Grest GS, Svaneborg C, Sivasubramanian A, Kremer K. Science 2004;303(5659):823–6.